

Learning Treatment Policies From Multimodal Electronic Health Records

Henri Arno

Department of Information Technology, Ghent University - imec, Ghent, Belgium

HENRI.ARNO@UGENT.BE

Thomas Demeester

Department of Information Technology, Ghent University - imec, Ghent, Belgium

THOMAS.DEMEESTER@UGENT.BE

Abstract

We study how to learn effective treatment policies from multimodal electronic health records (EHRs) that consist of tabular data and clinical text. These policies can help physicians make better treatment decisions and allocate healthcare resources more efficiently. Causal policy learning methods prioritize patients with the largest expected treatment benefit. Yet, existing estimators assume tabular covariates that satisfy strong causal assumptions, which are typically violated in the multimodal setting. As a result, predictive models of baseline risk are commonly used in practice to guide such decisions, as they extend naturally to multimodal data. However, such risk-based policies are not designed to identify which patients benefit most from treatment. We propose an extension of causal policy learning that uses expert-provided annotations during training to supervise treatment effect estimation, while using only multimodal representations as input during inference. We show that the proposed method achieves strong empirical performance across synthetic, semi-synthetic, and real-world EHR datasets, thereby offering practical insights into applying causal machine learning to realistic clinical data.

Data and Code Availability. This study uses both semi-synthetic and real-world data derived from the MIMIC-III database (Johnson et al., 2016), and from the fully synthetic SYN-SUM dataset (Rabaey et al., 2024). All code required to generate the data and reproduce the experiments is available at <https://anonymous.4open.science/r/causal-ehr>.

Institutional Review Board (IRB). This study does not involve human subjects research and therefore did not require Institutional Review Board (IRB) approval.

1. Introduction

Machine learning (ML) is increasingly being used in healthcare to support clinical decision-making (Esteva et al., 2019; Rajkomar et al., 2019). A central problem in this context, is learning from observational data which patients should receive treatment, supporting more targeted and efficient allocation of clinical resources (Athey and Wager, 2021; Nie et al., 2021). Electronic health records (EHRs) are widely available in modern healthcare systems and capture rich, patient-specific information, making them well suited for learning data-driven treatment policies (Tang et al., 2024; Shickel et al., 2017). However, these records are typically multimodal, combining tabular data and clinical text. In this work, *we study how to learn effective treatment policies from such multimodal EHR data.*

One strategy to tackle this problem, is to directly estimate treatment effects and prioritize patients with the largest expected benefit (Feuerriegel et al., 2024; Bica et al., 2021). By explicitly modeling how outcomes change under different treatment assignments, this strategy directly aligns the learning objective with the goal of making effective treatment decisions. However, existing estimators typically assume tabular covariates that satisfy strong causal identification assumptions, such as unconfoundedness. These conditions are difficult to satisfy in practice, particularly in EHRs where patient information is distributed across multiple modalities, such as tabular data and clinical text.

Because of these challenges, a more common strategy in practice is predictive modeling of the clinical outcome in absence of treatment (Van Smeden et al., 2021; Goldstein et al., 2016). The resulting predictions form an estimate of the patients’ so-called *baseline risk* and treatment can be prioritized for those most at risk. This approach is appealing because predictive models can easily handle multimodal data, and richer data often translate into higher predictive accuracy. However, as these models do not target treatment effects directly, they may fail to identify the patients who would benefit most, leading to suboptimal treatment allocation.

Proposed Method. We extend the causal strategy to the multimodal setting by estimating treatment effects from pre-trained representations of the data. The method builds on the doubly robust learner (Kennedy, 2023) to estimate *coarsened* effects, which quantify the expected treatment benefit given the information contained in these representations. At inference time, the model relies only on the representations to assign the treatments. During training, we assume access to expert-provided annotations to supervise the treatment effect estimation. These annotations should capture the clinical factors influencing both treatment and outcome and provide the information needed to adjust for confounding.

Main Results. Our experiments indicate that the representation-based coarsened effects can be learned reliably from multimodal data given suitable supervision, with estimation quality improving as more annotated data become available. Across synthetic and semi-synthetic benchmarks, the proposed causal policies match or exceed the performance of risk-based policies, depending on how baseline risk (mis)aligns with treatment benefit in the dataset. On real-world clinical data, substantially different treatment assignments are found for the causal vs. risk-based policies, confirming that naively pursuing risk-based modeling may not be the best strategy in the multimodal setting.

Contributions. Together, these findings motivate the following three key contributions:

- We study the problem setting of learning treatment policies from multimodal EHR

data, where patient information is distributed across multiple modalities, leading to violations of standard causal assumptions.

- We introduce a method for causal policy learning on multimodal data, estimating treatment effects from pre-trained representations at inference, while relying on expert-provided annotations during training.
- We empirically evaluate, analyze, and discuss the proposed causal method across synthetic, semi-synthetic, and real-world clinical datasets, comparing causal and risk-based treatment policies in terms of performance and treatment assignment.

2. Background and Related Work

We summarize the foundations of learning treatment policies from observational data and outline existing strategies for this task. An additional related work section is provided in Appendix A.

2.1. Learning Treatment Policies From Observational Data.

Consider a setting where each individual i in the considered population is characterized by covariates X_i , receives a binary treatment $T_i \in \{0, 1\}$, and has an associated continuous outcome $Y_i \in \mathbb{R}$. In the Rubin-Neyman potential outcomes framework (Rubin, 2005), each individual also has two potential outcomes, $Y_i(1)$ and $Y_i(0)$, where $Y_i(t)$ denotes the outcome that we would observe if individual i were assigned treatment $T_i = t$. In practice, only one of the two potential outcomes is observed, corresponding to the treatment that was actually received.

A *treatment policy* π is a rule that maps individual covariates to a treatment decision $\pi(x) : \mathcal{X} \rightarrow \{0, 1\}$. In the potential outcomes framework, the performance of a policy can be quantified by its *policy value*,

$$\begin{aligned} V(\pi) &= \mathbb{E}[Y(\pi(X))] \\ &= \mathbb{E}[\pi(X)Y(1) + (1 - \pi(X))Y(0)], \end{aligned}$$

which represents the mean outcome in the population if treatment were assigned according to π .

The optimal policy π^* is the one that maximizes the policy value (assuming larger outcomes are better). In many applications, however, treatment resources are limited and only k individuals out of a population *can* be treated. In such constrained settings, the optimal policy maximizes the policy value while satisfying the resource constraint.

In practice, we aim to learn treatment policies from observed data $(X, T, Y) \sim P$, where the joint distribution factorizes as $P(X, T, Y) = P(X)P(T | X)P(Y | X, T)$. Here, $P(T | X)$ represents the existing, possibly suboptimal, *observational policy* $\pi_{\text{obs}}(x)$. The goal of treatment policy learning is to use this data to estimate a new policy $\hat{\pi}$ that achieves a higher policy value than π_{obs} and approximates π^* .

2.2. Causal Treatment Policies.

Causal strategies learn treatment policies by modeling how outcomes would change under different treatment assignments. Within this framework, two main approaches have emerged. First, in *direct policy learning*, the treatment policy is learned directly by optimizing an empirical estimate of the policy value (Qian and Murphy, 2011; Kallus, 2018; Athey and Wager, 2021). Second, in *CATE-based policy learning*, the conditional average treatment effect (CATE) is estimated first, and individuals whose estimated benefit exceeds a threshold are treated (Fernández-Loría and Provost, 2022; Frauen et al., 2025). We focus on this latter family because it forms the basis of our proposed method.

The conditional average treatment effect (CATE) quantifies the expected benefit of treatment for an individual with covariates $X = x$,

$$\tau^x(x) = \mathbb{E}[Y(1) - Y(0) | X = x].$$

Because the CATE is not directly observable, we rely on the following standard causal inference assumptions for its identification:

- **Assumption 1.1 (consistency).** The observed outcome equals the potential outcome under the received treatment: $Y(t) = Y$ whenever $T = t$.
- **Assumption 1.2 (positivity):** Each individual has a non-zero probability of receiving either treatment: $0 < e(x) < 1$ where

$e(x) = \pi_{\text{obs}}(x) = P(T = 1 | X = x)$ is the *propensity score*.

- **Assumption 1.3 (unconfoundedness):** There are no unmeasured confounders: $Y(t) \perp\!\!\!\perp T | X$.

Under these assumptions, the CATE is identified, meaning that it can be estimated from observational data, and it may be expressed as

$$\begin{aligned} \tau^x(x) &= \mathbb{E}[Y | T=1, X=x] - \mathbb{E}[Y | T=0, X=x] \\ &= \mu_1(x) - \mu_0(x) \end{aligned}$$

where $\mu_t(x) = \mathbb{E}[Y | T = t, X = x]$ are the conditional mean outcomes under the treatments $t \in \{0, 1\}$, referred to as the *response surfaces*.

There is a rich literature on estimating the CATE from observational data. Existing machine learning models have been adapted for this purpose, including Gaussian processes, random forests, and generative adversarial networks (Alaa and van der Schaar, 2017; Wager and Athey, 2018; Yoon et al., 2018). Recently, meta-learners have gained popularity as they decompose effect estimation into subproblems that can each be solved with conventional supervised learners (Künzel et al., 2019; Nie and Wager, 2020; Kennedy, 2023). However, these estimators typically assume tabular covariates that satisfy the identifiability assumptions listed above, conditions that may be violated in multimodal clinical data. Recent work has begun to explore causal inference with representations of multimodal data, which we review in Appendix A.

2.3. Risk-Based Treatment Policies

An alternative strategy for learning treatment policies is to rely on *predictive* or *risk-based* models that estimate an individual’s expected outcome in the absence of treatment, $\mu_0(x) = \mathbb{E}[Y | T = 0, X = x]$. This quantity can then be interpreted as an individual’s baseline risk, and individuals with the highest predicted risk may be prioritized for treatment. Recent work has examined how these strategies compare to causal methods (Fernández-Loría and Provost, 2022; Fernández-Loría et al., 2023; Athey et al., 2025), and show that risk-based policies *can* perform competitively, for instance when treatment effects and baseline risk are strongly correlated, or

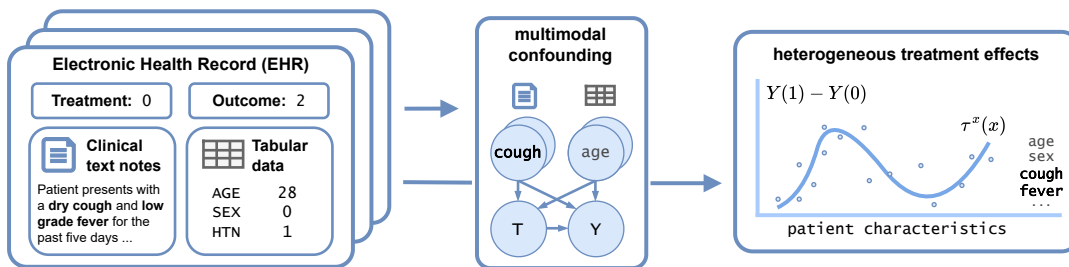


Figure 1: Overview of the problem setting. **Left:** Electronic health records combine tabular data and clinical text: key confounders (e.g., *cough*, *fever*) may appear only in text. **Middle:** Multimodal confounders influence both treatment T and outcome Y . **Right:** Heterogeneity in the conditional average treatment effect $\tau^x(x) = \mathbb{E}[Y(1) - Y(0) \mid X = x]$ across patient characteristics.

treatment effects are difficult to estimate due to small sample sizes.

This strategy is particularly appealing in the multimodal setting, as it does not rely on causal identification assumptions, and predictive accuracy often improves with richer data. For instance, clinical outcome prediction can drastically improve by relying on the multimodal data in electronic health records (Liu et al., 2018; Yang and Wu, 2021). However, while these models can predict outcomes well, our goal is to learn effective treatment policies rather than optimizing predictive accuracy.

3. Problem Setting

In this section, we describe the structure of the multimodal electronic health records considered in this work and how expert annotations can address the confounding challenges they introduce.

3.1. Multimodal EHR Data

Electronic health records (EHRs) are routinely collected in healthcare systems and capture detailed patient information, offering an opportunity to learn effective treatment policies from real-world data. These records typically combine tabular variables, such as demographics and lab measurements, with clinical text such as nursing notes describing patient symptoms, or radiology reports covering imaging results (Johnson et al., 2016). Because of this multimodality, clinical factors that influence both treatment decisions and patient outcomes may appear only in the text, as illustrated in Figure 1. In order to accurately es-

timate heterogeneous treatment effects from such data, it is therefore necessary to adjust for confounders that are distributed across the modalities.

3.2. Confounding Adjustment With Expert-Provided Annotations

The clinical notes in an EHR can be represented using a pre-trained encoder, such as ModernBERT (Warner et al., 2024), that maps each text to an embedding. These embeddings, once concatenated with the tabular variables, form a multimodal representation ϕ of each medical record. However, when the text only partially captures the confounding factors, or when the encoder does not fully preserve this information, the unconfoundedness assumption introduced in Section 2 is violated. In this scenario, the causal effects are not identifiable and cannot be estimated from observational data (ϕ, T, Y) alone.

To overcome this limitation, we assume that expert-provided annotations can be obtained for the confounders expressed in the text. These annotations require domain expertise to identify which factors in the multimodal data influence both treatment and outcome. In practice, this could involve a one-time annotation effort by medical experts to record this information in a structured way during their routine documentation. For instance, clinicians can record the presence of symptoms when writing patient reports, and radiologists can annotate imaging findings with tumor presence or suspected malignancy indicators when summarizing the results. Alternatively, these annotations may be collected retro-

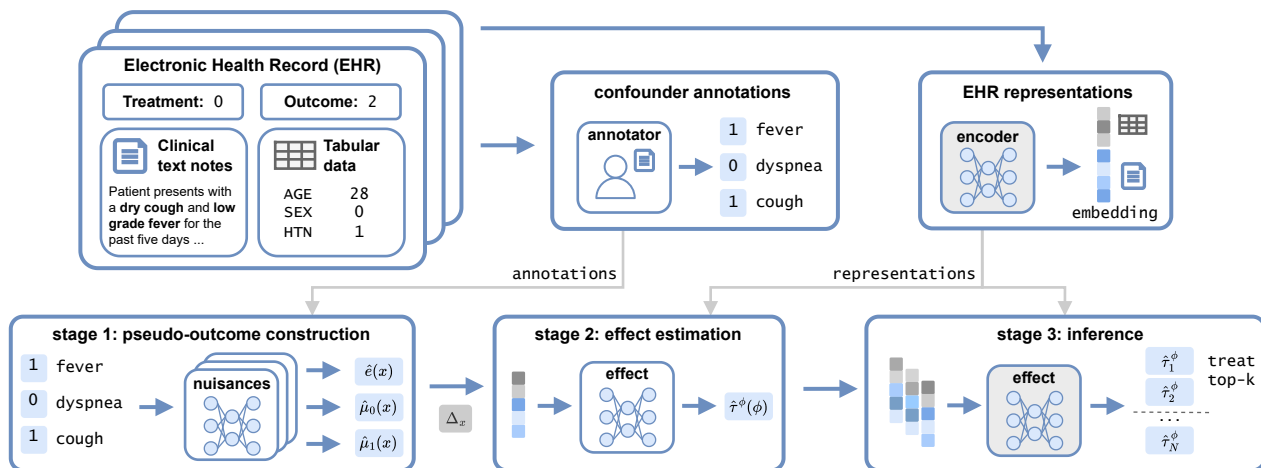


Figure 2: Overview of the proposed method. **Top:** Multimodal electronic health records are (1) annotated by experts to identify confounders and (2) encoded into joint representations using a pre-trained model. **Bottom:** The causal framework proceeds in three stages: (1) nuisance estimation and pseudo-outcome construction from annotated data, (2) effect estimation from multimodal representations, and (3) inference-time policy application based on the estimated coarsened effects.

spectively through expert review or with assistance from large language models to help generate or refine them (Ma et al., 2025). Formally, we assume that the annotated covariates X are sufficient to adjust for confounding ($Y(t) \perp\!\!\!\perp T \mid X$), alongside the standard assumptions of consistency and positivity. Consequently, the training data (ϕ, X, T, Y) includes annotations that provide supervision for treatment effect estimation during training. At inference, these annotations are not available, and treatment decisions must rely only on the representations. This setup is illustrated in the top row of Figure 2.

4. Proposed Method

We next present our method, shown in Figure 2, for learning treatment policies from multimodal EHR data. We motivate coarsened treatment effects as the target estimand and show how they can be estimated and used during inference.

4.1. Coarsened Treatment Effects

We propose to learn treatment policies based on *coarsened treatment effects*, defined as the expected treatment benefit conditional on the mul-

timodal representation ϕ of an EHR

$$\begin{aligned} \tau^\phi(\phi) &:= \mathbb{E}[Y(1) - Y(0) \mid \phi] \\ &= \int \tau^x(x) p(x \mid \phi) dx. \end{aligned}$$

Intuitively, $\tau^\phi(\phi)$ averages the treatment effects $\tau^x(x)$ over the patient subgroups whose covariates are consistent with the representation. It interpolates between the ATE when the representation is uninformative about the covariates, and the CATE when it perfectly captures them. Note that the equality above follows from the law of iterated expectations under the assumption that the representations provide no additional information about the potential outcomes beyond the covariates ($Y(t) \perp\!\!\!\perp \phi \mid X$ for $t \in \{0, 1\}$). This assumption is reasonable in our setting, since the representations are derived from clinical text describing the underlying covariates.

Treatment Policies Based on Coarsened Effects. As discussed in Section 2.2, CATE-based policies depend only on the ordering of treatment effects and allocate treatment to the individuals with the highest expected treatment benefit. When the multimodal representations lose confounding information, the coarsened effects $\tau^\phi(\phi)$ may differ from the true effects $\tau^x(x)$.

Nonetheless, if the coarsening bias remains limited, the coarsened effects can still be used to learn an optimal policy.

To see this, consider the coarsening bias

$$\delta_i = |\tau^x(x_i) - \tau^\phi(\phi_i)|,$$

which quantifies how much the coarsened effect differs from the true effect for individual i , and the margin

$$\gamma_i = \min_{x' \neq x_i} |\tau^x(x_i) - \tau^x(x')|,$$

which measures how distinct the treatment effect of individual i is from the effects of others in the considered population.

These quantities provide intuition for when coarsened effects can still be used for policy learning. If the coarsening bias δ_i is small relative to the margins γ_i , then coarsening does not alter the relative ordering of treatment effects in the population. In this case, ranking individuals according to the coarsened effects $\tau^\phi(\phi)$ results in the same treatment assignments as ranking by the true effects $\tau^x(x)$, and the implied policy remains optimal for any choice of treatment budget k . Figure 3 illustrates the setting where coarsening shifts the effect values but preserves their ordering.

If we consider a fixed treatment budget k , the requirements become even less strict. In this case, it is not necessary to preserve the full ordering of treatment effects, it suffices that the separation between individuals in the top- k and those ranked lower is maintained. Even if the coarsening bias distorts the ordering within the treated or untreated groups, the resulting policy remains optimal as long as no individuals are swapped across this treatment decision boundary.

Note that in practice, there is no straightforward way to verify whether coarsening preserves treatment effect ordering, as this would require knowledge of the true treatment effects, similar to the standard identification assumptions discussed in Section 2.2. However, if the covariates X can be recovered reasonably well from the representations ϕ in the training data, this provides an indication that the coarsening bias is small and unlikely to affect the treatment decisions.

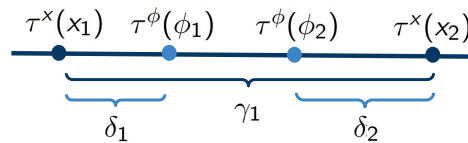


Figure 3: **Preservation of treatment effect ordering.** When the coarsened effects differ from the true effects, because the representations lose some confounding information, the ordering of individuals in the population, and the implied treatment policy, could nevertheless remain unchanged. This is the case, as long as the coarsening bias (δ_i) is small relative to the gaps between the true treatment effects (γ_i).

4.2. Learning Treatment Policies Based on Coarsened Effects

The proposed method proceeds in three stages, as shown in the bottom row of Figure 2 and discussed in detail below.

Stage 1: Pseudo-Outcome Construction.

The method builds on the doubly robust (DR) learner, a standard meta-learner for estimating the conditional average treatment effect (Kennedy, 2023). First, we construct a *pseudo-outcome* that provides an unbiased approximation of the treatment effect $\tau^x(x)$. This pseudo-outcome depends on estimates of the propensity score $\hat{e}(x)$ and the response models $\hat{\mu}_t(x)$, fitted on the annotated data, and is given by

$$\Delta_x = \hat{\mu}_1(x) - \hat{\mu}_0(x) + \frac{T - \hat{e}(x)}{\hat{e}(x)(1 - \hat{e}(x))} (Y - \hat{\mu}_t(x)).$$

By the doubly robust property, whenever the propensity model *or* the outcome models are correctly specified, this pseudo-outcome is unbiased for the treatment effect $\mathbb{E}[\Delta_x | X = x] = \tau^x(x)$.

Stage 2: Effect Estimation.

In the second stage, we estimate the coarsened treatment effects by regressing the pseudo-outcomes on the multimodal representations. This step is justified by the law of iterated expectations, which implies that the expected pseudo-outcomes given the representations equals the target estimand, $\mathbb{E}[\Delta_x | \phi] = \tau^\phi(\phi)$. In this step, the model learns how treatment benefit varies with the information encoded in the representations.

Stage 3: Inference. During inference, all electronic health records from the target population are encoded into their multimodal representations. The trained effect model from the previous stage then predicts the coarsened treatment effect for each record based on these representations alone, without requiring any annotations. Then, we rank patients directly by their predicted effects and assign treatment to the top- k . We consider only settings in which treatment is not harmful, as required by the ranking-based treatment assignment.

5. Experimental Results

We empirically evaluate the proposed method on synthetic, semi-synthetic, and real-world datasets to assess its effectiveness for policy learning from multimodal EHR data. Full details on the benchmark datasets and the experimental settings are provided in Appendices B, C and D.

5.1. Datasets

We evaluate our method on three datasets of electronic health records, ranging from fully synthetic to real-world data, which together enable a controlled, yet realistic evaluation.

Synthetic – SynSum. The fully synthetic SYNSUM dataset consists of 10,000 medical records that contain tabular variables and free-text clinical notes (Rabaey et al., 2024). The notes were generated with an LLM and describe patient symptoms such as fever, cough, or pain, which act as confounders influencing both the antibiotics treatment and the outcome. In this dataset, expert annotations were simulated by using the true symptom values that were used to generate the text. This benchmark provides realistic multimodal EHR data with known ground-truth effects, enabling controlled evaluation of the proposed causal policy learning method.

Semi-Synthetic – MIMIC-Syn. The semi-synthetic MIMIC-SYN benchmark was derived from the publicly available MIMIC-III database of intensive care EHRs (Johnson et al., 2016). Following Chen et al. (2024), we retain the real clinical notes and demographic variables but simulate treatment and outcome variables based on

cardiovascular diagnoses, age, and sex. The diagnosis indicators act as confounders, influencing both treatment and outcome, that are implicitly captured in the clinical text. During training, the true diagnosis indicators were used to simulate the expert annotations. This setup preserves the realism of clinical data while also providing a known causal ground truth for evaluation.

Real-World – MIMIC-Real. The dataset MIMIC-REAL was derived from the MIMIC-III database as well (Johnson et al., 2016). It consists of the multimodal EHRs from intensive care patients, where the treatment corresponds to antibiotics administration between three and nine hours after ICU admission and the outcome is in-hospital mortality. Each record combines tabular demographic variables with clinical notes documented prior to treatment, capturing the state of the patient before the decision to administer antibiotics. Vital-sign measurements were used to simulate the expert-provided annotations during training, as they strongly influence both antibiotics prescription and mortality risk. As in any observational dataset, the unconfoundedness assumption (given the annotations) cannot be verified. By consequence, this dataset allows us to compare different treatment assignment strategies qualitatively, but no quantitative evaluation is possible since ground-truth effects remain unknown.

5.2. Confounder Signal in Text

Throughout we have assumed that the multimodal EHR representations capture the confounding information expressed in the clinical text, even if this information is only partially preserved. To verify this in practice, we evaluate how well the annotated confounders can be recovered from the text embeddings across all datasets. Table 1 illustrates this for the semi-synthetic MIMIC-SYN dataset, where the cardiovascular diagnoses serve as the confounders implicitly encoded in the text. It is clear that all four diagnoses are predictable from the text, although with varying degrees of accuracy. Similar trends were observed for the other datasets, with slightly stronger recoverability of the confounders in SYNSUM and more modest performance in MIMIC-REAL (Appendix C). These results confirm that the representations capture the

Table 1: Prediction of diagnostic confounders from clinical notes in the MIMIC-SYN dataset (mean \pm std over 5 random seeds). “Prev.” denotes the positive-class prevalence in the test set. Each classifier’s decision threshold was selected to maximize F1 score on the validation set.

Confounder	Prev.	F1	Acc.	AUPRC	AUROC
Atrial fibrillation	0.24	0.694 \pm 0.007	0.856 \pm 0.005	0.759 \pm 0.004	0.889 \pm 0.002
Congestive heart failure	0.22	0.591 \pm 0.005	0.794 \pm 0.009	0.584 \pm 0.004	0.845 \pm 0.002
Coronary atherosclerosis	0.26	0.766 \pm 0.003	0.884 \pm 0.006	0.854 \pm 0.004	0.917 \pm 0.002
Hypertension	0.44	0.648 \pm 0.002	0.573 \pm 0.009	0.615 \pm 0.002	0.694 \pm 0.002

clinical confounding factors, supporting their use for estimating coarsened treatment effects. Additionally, the ability to recover confounders from the text suggests that the coarsening bias in the treatment effects, discussed in Section 4.1, will remain limited and is therefore unlikely to change the implied treatment policies substantially.

5.3. Coarsened Treatment Effect Quality

We next assess how well the coarsened treatment effects can be learned from the multimodal EHR representations on the datasets where ground-truth effects are available. We trained models to estimate treatment effects using varying amounts of training data and evaluated them using PEHE (the precision in estimation of heterogeneous effects), defined as the root mean squared error between the estimates and the true treatment effects. We trained the second-stage treatment effect models in three scenarios: using the true confounders, the multimodal representations (text + tabular) and the tabular variables only as inputs. Note that in all three scenarios the same pseudo-outcomes are used as targets, which are based on the nuisance models fitted on the annotations.

Figure 4 illustrates the results on the SYN-SUM dataset (similar results for MIMIC-SYN are reported in Appendix C). Across inputs, treatment effect estimation improves with more training data. The models based on true confounders perform best, followed by the multimodal models and the tabular-only models. This indicates that while the multimodal representations introduce coarsening (text + tabular vs. true confounders), incorporating the clinical text does help to recover more accurate treatment effects compared to tabular-only inputs (text + tabular vs. tabular).

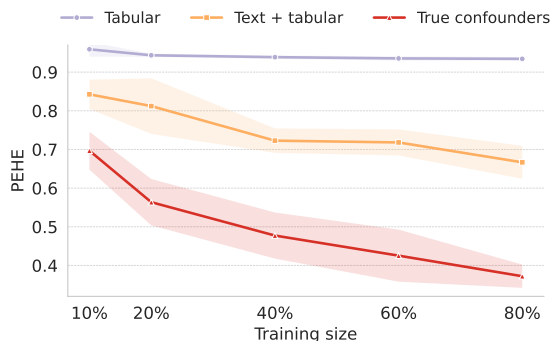


Figure 4: Precision in estimation of heterogeneous effects (PEHE) on the SYN-SUM dataset as a function of training set size (mean \pm std over 5 random seeds). The second-stage treatment effect models were trained and evaluated with the true confounders, the multimodal representations (text + tabular) and the tabular variables only as inputs.

5.4. Treatment Policy Evaluation

We next evaluate the performance of the proposed method for learning treatment policies. Specifically, we compare the causal policy derived from the estimated coarsened treatment effects to a standard risk-based policy that assigns treatment according to the predicted baseline risk. We first assess both strategies quantitatively on the synthetic and semi-synthetic datasets, where ground-truth effects are available, and then compare them qualitatively on the real-world data to examine how their treatment assignment differs in practice.

Table 2: Policy evaluation metrics on the SYNSUM and MIMIC-SYN datasets (mean \pm std over five random seeds). Lower policy values (indicated as \bar{V} for mean policy value over all thresholds, and $V_{10\%}$ at the 10% threshold) and more negative AUTOOC indicate better performance. The best model within each training size is shown in **bold**, unless the difference was not significant at the 5% level based on a two-sided t -test. The ‘‘oracle’’ row report the metrics of policies ranking by the true treatment effect (causal) or the untreated outcome (risk-based).

Dataset	Training Size	Model	AUTOOC (\downarrow)	\bar{V} (\downarrow)	$V_{10\%}$ (\downarrow)
SYNSUM	40%	Causal	-0.61 ± 0.06	1.747 ± 0.005	1.822 ± 0.015
		Risk-Based	-0.67 ± 0.02	1.746 ± 0.002	1.812 ± 0.006
	80%	Causal	-0.65 ± 0.06	1.742 ± 0.003	1.814 ± 0.018
		Risk-Based	-0.68 ± 0.00	1.745 ± 0.000	1.812 ± 0.002
	Oracle	Causal	-0.88	1.697	1.766
		Risk-Based	-0.81	1.724	1.784
MIMIC-SYN	40%	Causal	-0.14 ± 0.00	1.049 ± 0.001	1.368 ± 0.001
		Risk-Based	0.17 ± 0.00	1.150 ± 0.000	1.428 ± 0.001
	80%	Causal	-0.14 ± 0.00	1.047 ± 0.001	1.368 ± 0.000
		Risk-Based	0.18 ± 0.00	1.152 ± 0.001	1.429 ± 0.000
	Oracle	Causal	-0.20	1.020	1.362
		Risk-Based	0.28	1.172	1.450

Evaluation Metrics. For the datasets with known ground-truth effects (SYNSUM and MIMIC-SYN), we evaluate each policy using three complementary metrics and under varying treatment budgets. Both the causal and risk-based strategies produce a ranking of individuals in the test population, either by the estimated coarsened treatment effect or by the predicted baseline risk. For a given treatment budget k , corresponding to a fraction of the population that can be treated, we evaluate the policy obtained by treating the top- k individuals in this ranking.

Following the definition introduced in Section 2, the policy value $V(\pi)$ measures the expected outcome in the population if treatment were assigned according to a given policy π . We report the policy value for the constrained case with a budget of $k=10\%$ as $V_{10\%}$ and the mean policy value averaged across all treatment budgets k as \bar{V} . In addition, we report the AUTOOC (area under the treatment-outcome curve) (Yadlowsky et al., 2025), which measures the average benefit from treating individuals prioritized by the model, averaged across all treatment budgets k and relative to the average treatment ef-

fect (ATE). Lower AUTOOC values indicate that the policy more effectively concentrates treatment benefit among the top-ranked individuals.

Benchmarking Results. Table 2 compares the causal and risk-based policies across training sizes for the fully synthetic SYNSUM and semi-synthetic MIMIC-SYN datasets (extended results are provided in Appendix C). On the SYNSUM dataset, both the causal and risk-based policies achieve comparable performance across all metrics and approach their respective oracle values as the amount of annotated training data increases. In contrast, on the MIMIC-SYN dataset, the causal policy consistently outperforms the risk-based policy. This difference arises from how baseline risk aligns with treatment benefit in each dataset. In SYNSUM, the two are positively correlated, which means that patients at higher risk also experience greater treatment benefit, so prioritizing by predicted risk or by estimated effect leads to similar treatment assignments. In MIMIC-SYN, the relationship is reversed as high-risk patients benefit less from treatment causing the risk-based policy to misallocate treatment toward individuals with

Table 3: Agreement in treatment recommendations between the causal and risk-based policies on the MIMIC-REAL dataset (mean \pm std over five random seeds). Each value reports the percentage of patients jointly prioritized by both policies at a given top- k % treatment budget, with higher values indicating higher agreement in treatment prioritization.

Top- k (%)	Agreement (%) (Causal vs. Risk-Based)
$k = 5$	5.0 ± 7.0
$k = 10$	13.8 ± 8.0
$k = 20$	24.4 ± 7.8
$k = 50$	53.0 ± 5.3
$k = 100$	100.0 ± 0.0

small effects. The relationship between baseline risk and treatment benefit is visualized in Appendix C, Figure 5.

Real-World Treatment Allocation. Finally, we compare the treatment recommendations generated by the causal and risk-based policies on the real-world MIMIC-REAL dataset, where ground-truth treatment effects are unknown. As shown in Table 3, the overlap between the two policies is limited. For instance, only about 25% of the patients prioritized in the top 20% by either strategy are shared, indicating that the policies target largely distinct patient subgroups. Additionally, we compared the learned policies with the observed antibiotic prescription policy in the data (see Appendix C, Table 10). While the risk-based policy showed slightly higher agreement with the observed prescriptions than the causal policy, the overlap with the observed prescriptions was generally low for both strategies. These findings highlight that the different methods may generate substantially different treatment assignments in practice.

5.5. Discussion and Limitations

Across all experiments, we showed that coarsened treatment effects can be estimated reliably from multimodal electronic health records given suitable supervision. In the controlled synthetic settings, the proposed causal policy learning method

matched or exceeded risk-based policies, depending on how baseline risk and treatment benefit were correlated in the data. On real-world EHR data, the two strategies prioritized different patient subgroups, highlighting the importance of choosing an appropriate policy learning method.

While these results demonstrate the potential of causal policy learning from multimodal EHRs, several limitations should be noted. First, the method requires confounder annotations during training to supervise treatment effect estimation. Obtaining such annotations may be difficult in practice, yet without them, the treatment effects are not identifiable from the observational data alone. Second, whether the coarsened effects preserve the treatment effect ordering cannot be tested on real-world data, as it depends on the unknown true treatment effects. However, evaluating how well the confounders can be recovered from the representations gives an empirical indication of whether the coarsening bias will affect the implied treatment policy. Finally, in our (semi-)synthetic experiments, the expert-provided annotations were simulated using the ground-truth confounders, representing the ideal scenario. Future work should investigate how the method performs when using annotations collected from human experts or derived from auxiliary models.

6. Conclusion

We studied how to learn effective treatment policies from multimodal electronic health records that combine tabular data and clinical text. While risk-based models are commonly used to guide clinical decisions, they do not explicitly target treatment benefit. We proposed a causal policy learning approach that estimates coarsened treatment effects using expert-provided annotations during training and relies only on multimodal representations at inference. The method is theoretically justified and empirically effective, resulting in competitive treatment policies on synthetic and semi-synthetic data and qualitatively different treatment assignments on real-world EHR data. These findings highlight the feasibility of causal policy learning from multimodal data and provide practical insights for applying causal machine learning to realistic health-care settings.

References

- Ahmed Alaa and Mihaela van der Schaar. Bayesian inference of individualized treatment effects using multi-task gaussian processes. In *Advances in Neural Information Processing Systems*, 2017.
- Susan Athey and Stefan Wager. Policy learning with observational data. *Econometrica*, 89(1), 2021.
- Susan Athey, Niall Keleher, and Jann Spiess. Machine learning who to nudge: Causal vs predictive targeting in a field experiment on student financial aid renewal. *Journal of Econometrics*, 249, 2025.
- Ioana Bica, Ahmed Alaa, Craig Lambert, and Mihaela Van Der Schaar. From real-world patient data to individualized treatment effects using machine learning: current and future methods to address underlying challenges. *Clinical Pharmacology & Therapeutics*, 109(1), 2021.
- Jacob Chen, Rohit Bhattacharya, and Katherine Keith. Proximal causal inference with text data. In *Advances in Neural Information Processing Systems*, 2024.
- Alicia Curth and Mihaela van der Schaar. On inductive biases for heterogeneous treatment effect estimation. In *Advances in Neural Information Processing Systems*, 2021.
- Adel Daoud, Connor Jerzak, and Richard Johansson. Conceptualizing treatment leakage in text-based causal inference. In *The North American Chapter of the Association for Computational Linguistics: Human Language Technologies*, 2022.
- Naoki Egami, Christian Fong, Justin Grimmer, Margaret Roberts, and Brandon Stewart. How to make causal inferences using texts. *Science Advances*, 8(42), 2022.
- Andre Esteva, Alexandre Robicquet, Bharath Ramsundar, Volodymyr Kuleshov, Mark Depristo, Katherine Chou, Claire Cui, Greg Corrado, Sebastian Thrun, and Jeff Dean. A guide to deep learning in healthcare. *Nature medicine*, 25(1), 2019.
- Carlos Fernández-Loría and Foster Provost. Causal classification: Treatment effect estimation vs. outcome prediction. *Journal of Machine Learning Research*, 23(59), 2022.
- Carlos Fernández-Loría, Foster Provost, Jesse Anderton, Benjamin Carterette, and Praveen Chandar. A comparison of methods for treatment assignment with an application to playlist generation. *Information Systems Research*, 34(2), 2023.
- Stefan Feuerriegel, Dennis Frauen, Valentyn Melnychuk, Jonas Schweisthal, Konstantin Hess, Alicia Curth, Stefan Bauer, Niki Kilbertus, Isaac Kohane, and Mihaela van der Schaar. Causal machine learning for predicting treatment outcomes. *Nature Medicine*, 30(4), 2024.
- Dennis Frauen, Valentyn Melnychuk, Jonas Schweisthal, Mihaela van der Schaar, and Stefan Feuerriegel. Treatment effect estimation for optimal decision-making. In *Advances in Neural Information Processing Systems*, 2025.
- Benjamin Goldstein, Ann Marie Navar, Michael Pencina, and John Ioannidis. Opportunities and challenges in developing risk prediction models with electronic health records data: a systematic review. *Journal of the American Medical Informatics Association*, 24(1), 2016.
- Limor Gultchin, David Watson, Matt Kusner, and Ricardo Silva. Operationalizing complex causes: A pragmatic view of mediation. In *The International Conference on Machine Learning*, 2021.
- Connor Jerzak, Fredrik Johansson, and Adel Daoud. Image-based treatment effect heterogeneity. In *The Conference on Causal Learning and Reasoning*, 2023.
- Fredrik Johansson, Uri Shalit, and David Sontag. Learning representations for counterfactual inference. In *The International Conference on Machine Learning*, 2016.
- Fredrik Johansson, Uri Shalit, Nathan Kallus, and David Sontag. Generalization bounds and representation learning for estimation of potential outcomes and causal effects. *Journal of Machine Learning Research*, 23(166), 2022.

- Alistair Johnson, Tom Pollard, Lu Shen, Liwei Lehman, Mengling Feng, Mohammad Ghassemi, Benjamin Moody, Peter Szolovits, Leo Anthony Celi, and Roger Mark. MIMIC-III, a freely accessible critical care database. *Scientific Data*, 3(160035), 2016.
- Nathan Kallus. Balanced policy evaluation and learning. In *Advances in Neural Information Processing Systems*, 2018.
- Katherine Keith, David Jensen, and Brendan O’Connor. Text and causal inference: A review of using text to remove confounding from causal estimates. In *The Annual Meeting of the Association for Computational Linguistics*, 2020.
- Edward Kennedy. Towards optimal doubly robust estimation of heterogeneous causal effects. *Electronic Journal of Statistics*, 17(2), 2023.
- Sven Klaassen, Jan Teichert-Kluge, Philipp Bach, Victor Chernozhukov, Martin Spindler, and Suhas Vijaykumar. DoubleMLdeep: Estimation of causal effects with multimodal data, 2024. preprint - arXiv:2402.01785.
- Sören Künzel, Jasjeet Sekhon, Peter Bickel, and Bin Yu. Meta learners for estimating heterogeneous treatment effects using machine learning. *Proceedings of the National Academy of Sciences*, 116(10), 2019.
- Jingshu Liu, Zachariah Zhang, and Narges Razavian. Deep EHR: Chronic disease prediction using medical notes. In *Machine Learning for Healthcare Conference*, 2018.
- Yuchen Ma, Dennis Frauen, Jonas Schweisthal, and Stefan Feuerriegel. LLM-driven treatment effect estimation under inference time text confounding. In *Advances in Neural Information Processing Systems*, 2025.
- Valentyn Melnychuk, Dennis Frauen, and Stefan Feuerriegel. Bounds on representation-induced confounding bias for treatment effect estimation. In *The International Conference on Learning Representations*, 2024.
- Xinkun Nie and Stefan Wager. Quasi-oracle estimation of heterogeneous treatment effects. *Biometrika*, 108(2), 2020.
- Xinkun Nie, Emma Brunskill, and Stefan Wager. Learning when-to-treat policies. *Journal of the American Statistical Association*, 116(533), 2021.
- Min Qian and Susan Murphy. Performance guarantees for individualized treatment rules. *Annals of statistics*, 39(2), 2011.
- Paloma Rabaey, Henri Arno, Stefan Heytens, and Thomas Demeester. SynSum – Synthetic benchmark with structured and unstructured medical records. In *AAAI 2025 Workshop on GenAI4Health*, 2024.
- Alvin Rajkomar, Jeffrey Dean, and Isaac Kohane. Machine learning in medicine. *New England Journal of Medicine*, 380(14), 2019.
- Donald Rubin. Causal inference using potential outcomes. *Journal of the American Statistical Association*, 100(469), 2005.
- Pedro Sanchez and Sotirios Tsafaris. Diffusion causal models for counterfactual estimation. In *The Conference on Causal Learning and Reasoning*, 2022.
- Uri Shalit, Fredrik Johansson, and David Sontag. Estimating individual treatment effect: generalization bounds and algorithms. In *The International Conference on Machine Learning*, 2017.
- Claudia Shi, David Blei, and Victor Veitch. Adapting neural networks for the estimation of treatment effects. In *Advances in Neural Information Processing Systems*, 2019.
- Benjamin Shickel, Patrick James Tighe, Azra Bihorac, and Parisa Rashidi. Deep EHR: A survey of recent advances in deep learning techniques for electronic health record (EHR) analysis. *IEEE journal of biomedical and health informatics*, 22(5), 2017.
- Alice Tang, Sarah Woldemariam, Silvia Miramontes, Beau Norgeot, Tomiko Oskotsky, and Marina Sirota. Harnessing EHR data for health research. *Nature Medicine*, 30(7), 2024.
- Maarten Van Smeden, Johannes Reitsma, Richard Riley, Gary Collins, and Karel Moons. Clinical prediction models: diagnosis versus prognosis. *Journal of clinical epidemiology*, 132, 2021.

Victor Veitch, Dhanya Sridhar, and David Blei. Adapting text embeddings for causal inference. In *Uncertainty in Artificial Intelligence*, 2020.

Stefan Wager and Susan Athey. Estimation and inference of heterogeneous treatment effects using random forests. *Journal of the American Statistical Association*, 113(523), 2018.

Benjamin Warner, Antoine Chaffin, Benjamin Clavié, Orion Weller, Oskar Hallström, Said Taghadouini, Alexis Gallagher, Raja Biswas, Faisal Ladhak, Tom Aarsen, Nathan Cooper, Griffin Adams, Jeremy Howard, and Iacopo Poli. Smarter, better, faster, longer: A modern bidirectional encoder for fast, memory efficient, and long context finetuning and inference, 2024. preprint - arXiv:2412.13663.

Zach Wood-Doughty, Ilya Shpitser, and Mark Dredze. Challenges of using text classifiers for causal inference. In *Empirical Methods in Natural Language Processing*, 2018.

Steve Yadlowsky, Scott Fleming, Nigam Shah, Emma Brunskill, and Stefan Wager. Evaluating treatment prioritization rules via rank-weighted average treatment effects. *Journal of the American Statistical Association*, 120(549), 2025.

Bo Yang and Lijun Wu. How to leverage the multimodal EHR data for better medical prediction. In *Empirical Methods in Natural Language Processing*, 2021.

Jinsung Yoon, James Jordon, and Mihaela van der Schaar. GANITE: Estimation of individualized treatment effects using generative adversarial nets. In *The International Conference on Learning Representations*, 2018.

Fucheng Warren Zhu, Connor Jerzak, and Adel Daoud. Optimizing multi-scale representations to detect effect heterogeneity using earth observation and computer vision: Application to two anti-poverty rcts. In *The Conference on Causal Learning and Reasoning*, 2025.

Appendix A. Additional Related Work

This appendix complements Section 2 by reviewing additional work on estimating treatment effects from high-dimensional representations or multimodal data. These studies have begun to explore CATE estimation beyond tabular covariates.

CATE Estimation With Learned Representations. Several authors have proposed neural network architectures that learn intermediate representations of tabular covariates for CATE estimation. Some of these models directly predict the potential outcomes (the *response surfaces*) from learned representations of the covariates, while constraining the induced representations so that their distributions are similar across treatment groups (Johansson et al., 2016; Shalit et al., 2017; Johansson et al., 2022). Other methods extend this idea by jointly predicting additional nuisance components, such as the propensity score, in order to improve the CATE estimates (Shi et al., 2019; Curth and van der Schaar, 2021). When these intermediate representations lose information on confounders, bias can arise in the resulting estimates, as studied by Melnychuk et al. (2024).

Causal Inference With Multimodal Data. Recent work has extended causal inference methods to multimodal data. Most studies have focussed on text (Wood-Doughty et al., 2018; Veitch et al., 2020; Keith et al., 2020; Gultchin et al., 2021; Daoud et al., 2022; Egami et al., 2022; Ma et al., 2025), with more recent efforts exploring images (Sanchez and Tsafaris, 2022; Jerzak et al., 2023; Zhu et al., 2025) and combinations of both (Klaassen et al., 2024). Depending on the application, the multimodal data may act as treatment, outcome, mediator, or confounder. Much of this work targets average treatment effects or uses representations of multimodal data as proxies for unobserved confounders. In contrast, we aim to estimate individualized (conditional) treatment effects from multimodal representations while leveraging expert-provided annotations during training to adjust for confounding.

Appendix B. Datasets

This appendix provides a detailed description of the datasets used in our experiments: the fully synthetic SYNSUM dataset (Rabaey et al., 2024), the semi-synthetic MIMIC-SYN dataset (Johnson et al., 2016; Chen et al., 2024), and the real-world MIMIC-REAL dataset (Johnson et al., 2016). For each synthetic dataset, we describe the data generating process, including the construction of treatments and outcomes. The MIMIC-REAL dataset is included only for a qualitative comparison of the treatment assignment strategies, without quantitative evaluation.

B.1. Synthetic – SynSum

The fully synthetic SYNSUM dataset (Rabaey et al., 2024)¹ consists of 10,000 medical patient records simulating primary care encounters for patients with respiratory diseases. Each record combines tabular variables with an associated free-text clinical note, mimicking the multimodal structure of real electronic health records (EHRs). The dataset is entirely specified and reproducible: tabular variables are sampled from a Bayesian network defined by a domain expert, while clinical notes are generated using GPT-4. SYNSUM thus provides realistic, simulated EHR data with ground-truth counterfactuals, enabling controlled evaluation of the considered treatment assignment strategies.

Tabular Variables. In SYNSUM, structured variables are first sampled from a Bayesian network that defines the underlying clinical relationships in the simulated population. The directed acyclic graph and the parameters of this Bayesian network were specified by a domain expert. The variables include diagnoses (pneumonia and common cold), symptoms (dyspnea, cough, pain, fever, nasal congestion), underlying respiratory conditions (asthma, smoking, chronic obstructive pulmonary disease, hay fever), and non-clinical factors (season, prescription policy, self-employment). Each variable is binary and can be represented by an indicator $x_{\text{var}} \in \{0, 1\}$. A detailed description of the Bayesian network and its parametrization is provided in Rabaey et al. (2024).

These structured variables serve different roles in the data generating process. A subset of them (self-employment status, smoking, winter season, asthma, chronic obstructive pulmonary disease, and hay fever) appear as tabular variables in the simulated EHRs, representing background and chronic-condition information typically recorded in structured fields. The symptom variables (dyspnea, cough, pain, fever, and nasal congestion) are used to generate the accompanying clinical text, where their presence or absence is expressed implicitly. Finally, a small number of variables (diagnoses and the policy indicator) are used solely to create realistic dependencies in the data but are not directly used elsewhere.

Treatment and Outcome. Based on the structured variables, we can simulate treatments and outcomes suitable for causal inference. The treatment variable $T \in \{0, 1\}$ indicates whether antibiotics were prescribed during the simulated consultation. It is sampled from a logistic regression model

$$P(T = 1 \mid X = x) = \sigma(-3 + 1.0 x_{\text{pol}} + 0.8 x_{\text{dysp}} + 0.665 x_{\text{cough}} + 0.665 x_{\text{pain}} + 0.9 x_{\text{f_low}} + 2.25 x_{\text{f_high}}),$$

where $\sigma(\cdot)$ denotes the sigmoid function. This specification reflects realistic clinical behaviour, where physicians are more likely to prescribe antibiotics in the presence of severe symptoms or under a permissive prescription policy.

The outcome variable Y represents the duration of illness (in days) and is modeled as a Poisson random variable conditioned on treatment,

$$P(Y = k \mid X = x, T = t) = \text{Poisson}(k \mid \lambda_t(x)),$$

where the Poisson rate parameters are defined as

$$\lambda_0(x) = \exp(0.010 + 0.64 x_{\text{dysp}} + 0.35 x_{\text{cough}} + 0.47 x_{\text{pain}} + 0.011 x_{\text{nasal}} + 0.81 x_{\text{f_low}} + 1.23 x_{\text{f_high}} - 0.5 x_{\text{self}}),$$

$$\lambda_1(x) = \exp(0.16 + 0.51 x_{\text{dysp}} + 0.42 x_{\text{cough}} + 0.26 x_{\text{pain}} + 0.0051 x_{\text{nasal}} + 0.24 x_{\text{f_low}} + 0.57 x_{\text{f_high}} - 0.5 x_{\text{self}}).$$

1. <https://github.com/prabaey/SimSum>

This formulation ensures that symptom severity acts as a confounder, influencing both treatment assignment and outcome. The ground-truth conditional average treatment effect (CATE) for each patient is given by $\tau^x(x) = \lambda_1(x) - \lambda_0(x)$.

Text Generation. Each record’s clinical note is generated by prompting a large language model (GPT-4) so that the patient’s symptoms are reflected in the text. The prompt design emphasizes clinical realism, coherence, and diversity in linguistic style to resemble documentation written at the time of consultation. In the final EHR, symptoms are not explicitly included in structured fields, instead, they are encoded implicitly in the free-text note. Each simulated EHR therefore consists of tabular background variables (e.g., smoking, chronic conditions, season) and a clinical note describing the patient’s symptoms in natural language.

Feature Representations. Each simulated EHR in SYNSUM consists of tabular background variables and a clinical text note. We encode the clinical text using the pretrained language model ModernBERT (Warner et al., 2024), mean-pool the token embeddings, and concatenate the resulting text representation with the tabular variables to obtain the multimodal representation ϕ . This representation captures both the tabular background information and confounding signal expressed implicitly in the text, reflecting the partial observability typical of real-world EHR data.

Confounding Annotations. Our causal modeling strategy assumes that domain experts can provide annotations on confounding information that is expressed in the clinical text. In SYNSUM, this process is simulated using the true values of the symptom variables (e.g., fever, cough, dyspnea), which influence both treatment and outcome. This setup enables controlled evaluation of the causal strategy that leverages expert-identified confounders during training while relying only on the multimodal representations at inference time.

Risk–Benefit Alignment. Finally, we characterize the relationship between baseline risk and treatment benefit by computing the Pearson correlation between the ground-truth base-

line outcome $\mu_0(x) = \mathbb{E}[Y \mid T = 0, X = x]$ and the true treatment effect $\tau^x(x) = \mathbb{E}[Y(1) - Y(0) \mid X = x]$. In this setting, the baseline outcome $\mu_0(x)$ equals the Poisson rate $\lambda_0(x)$. In SYNSUM, this correlation equals -0.91 , indicating a strong negative association: patients with higher baseline risk (larger $\mu_0(x)$) tend to experience larger treatment benefits (more negative $\tau^x(x)$). This property of the dataset implies that treatment assignment strategies based on predictive modeling of baseline risk may align well with the optimal policy. This relationship is visualized in Figure 5, together with the corresponding plot for MIMIC-SYN.

B.2. Semi-Synthetic – MIMIC-Syn

The semi-synthetic MIMIC-SYN dataset is derived from the publicly available MIMIC-III database (Johnson et al., 2016)², which contains de-identified electronic health records from over 35,000 intensive care unit (ICU) patients. The dataset includes both structured variables and free-text clinical notes. Following Chen et al. (2024), we retain the real tabular and textual features but generate synthetic treatment and outcome variables. This design preserves the realism of actual EHR data while enabling controlled evaluation under a known causal ground-truth.

Data Preprocessing. We follow the preprocessing pipeline of Chen et al. (2024) to construct patient-level records from the MIMIC-III database. Starting from all clinical notes, we remove entries with missing hospital admission IDs and exclude discharge summaries. For each patient (identified by a unique subject ID), we retain only the earliest hospital admission and concatenate all associated clinical notes into a single text sequence. Additionally, we extract basic demographic variables, age and sex, and retain them as tabular covariates in the EHR. Patients younger than 18 or older than 100 years are excluded. Each resulting record therefore consists of a single aggregated clinical note and a small set of tabular demographic attributes, forming a multimodal EHR with real-world patient data. Other structured variables from MIMIC-III are later used in the data generating process to con-

2. <https://physionet.org/content/mimiciii/1.4/>

struct treatment and outcome variables but are not directly included in the EHR.

Treatment and Outcome. To introduce heterogeneous treatment effects, we modify the setup of [Chen et al. \(2024\)](#) such that treatment is on average beneficial but less effective in severely ill patients. Treatment assignment and outcomes are simulated based on four cardiovascular diagnoses: hypertension, coronary atherosclerosis, atrial fibrillation, and congestive heart failure, together with patient age and sex. The diagnosis indicators ($x_{\text{var}} \in \{0, 1\}$) are extracted from the ICD-9 codes in the MIMIC-III tables, but are not included in the constructed EHRs. Prior analyses by [Chen et al. \(2024\)](#) showed that these diagnoses are among the most predictable conditions from clinical text, indicating that their information is implicitly encoded in the notes. Using these variables to generate treatments and outcomes therefore induces implicit confounding through the textual modality, analogous to the SYN-SUM setting.

The treatment variable $T \in \{0, 1\}$ indicates whether the hypothetical intervention was applied and is sampled from a logistic regression model

$$P(T = 1 \mid X = x) = \sigma(-1.2 + 0.2 x_{\text{hyp}} + 0.9 x_{\text{cor}} + 0.8 x_{\text{afib}} + 0.7 x_{\text{chf}} + 0.3 x_{\text{age}} + 0.2 x_{\text{sex}}),$$

where $\sigma(\cdot)$ denotes the sigmoid function. This specification reflects that patients with more cardiovascular risk factors or higher age are more likely to receive the treatment.

The continuous outcome Y represents an adverse clinical outcome (e.g., mortality risk or hospitalization days), where lower values indicate better outcomes. It is generated as

$$Y = 0.4 x_{\text{age}} + 0.6 x_{\text{sex}} + 0.2 x_{\text{hyp}} + 1.1 x_{\text{cor}} + 0.8 x_{\text{afib}} + 1.4 x_{\text{chf}} + T \cdot \tau^x(x) + \epsilon,$$

with $\epsilon \sim \mathcal{N}(0, 1)$ denoting standard Gaussian noise. The heterogeneous treatment effect function $\tau^x(x)$ captures that treatment benefit attenuates with disease severity and age, while varying smoothly across age groups

$$\tau^x(x) = -1 + 0.25 x_{\text{cor}} + 0.20 x_{\text{afib}} + 0.30 x_{\text{chf}} + 0.05 x_{\text{hyp}} + 0.35 x_{\text{cor}} x_{\text{afib}} + 0.05 x_{\text{chf}} x_{\text{hyp}} - 0.10 (1 - x_{\text{sex}}) + 0.10 \sin(\pi x_{\text{age}}).$$

Negative values of $\tau^x(x)$ indicate a beneficial effect (a reduction of the adverse outcome), while positive values correspond to harm. This specification ensures that treatment is beneficial on average (average treatment effect (ATE) ≈ -0.75), with attenuated benefit for older and sicker patients. This setup offers a semi-synthetic benchmark dataset that balances realism and interpretability, linking fully synthetic simulations with real-world EHR data.

Feature Representations. Each record in MIMIC-SYN consists of a clinical note and tabular demographic variables (age and sex). We encode the clinical text using the pretrained language model ModernBERT ([Warner et al., 2024](#)), mean-pool the token embeddings, and concatenate the resulting text representation with the tabular covariates to obtain the multimodal representation ϕ . This representation captures both demographic information and implicit confounding signal related to the latent cardiovascular diagnoses. Consequently, ϕ reflects a coarsened view of the underlying factors influencing treatment and outcome, again mirroring the partial observability typical of real-world EHR data.

Confounding Annotations. Our causal modeling strategy assumes that domain experts can provide annotations on confounding information that is expressed in the clinical text. In MIMIC-SYN, this process is simulated using the true cardiovascular diagnoses (hypertension, coronary atherosclerosis, atrial fibrillation, and congestive heart failure), which influence both treatment and outcome. These variables provide a supervision signal during training of the models, while relying only on the multimodal representations ϕ at inference time. This setup enables controlled evaluation of the causal approach that incorporates expert-identified confounding information in a semi-synthetic yet realistic setting.

Risk-Benefit Alignment. We characterize the relationship between baseline risk and treatment benefit by computing the Pearson correlation between the ground-truth baseline outcome $\mu_0(x) = \mathbb{E}[Y \mid T = 0, X = x]$ and the true treatment effect $\tau^x(x) = \mathbb{E}[Y(1) - Y(0) \mid X = x]$. In MIMIC-SYN, this correlation equals 0.94, indicating a strong positive relationship: patients

with higher baseline risk (larger $\mu_0(x)$) tend to experience smaller (or even adverse) treatment effects (less negative $\tau^x(x)$). Consequently, risk-based and causal treatment assignment strategies are not necessarily aligned in this dataset. The relationship between baseline risk and treatment benefit is visualized in Figure 5, together with the corresponding results for SYN-SUM.

B.3. Real-World – MIMIC-Real

We construct a real-world observational dataset from the MIMIC-III database (Johnson et al., 2016) to examine whether risk-based and causal treatment strategies diverge in actual clinical practice. In this setting, both the tabular variables and the clinical text notes of the electronic health records (EHRs) are derived directly from real-world patient data. The treatment (antibiotic administration) and the outcome (in-hospital mortality) are likewise observed rather than simulated. This dataset complements the synthetic and semi-synthetic analyses by extending the comparison of risk-based and causal policies to fully real-world clinical data. Because ground-truth counterfactuals are unavailable, we limit our analysis to a qualitative comparisons of treatment assignment under both strategies.

Data Preprocessing. We construct a patient-level dataset of electronic health records (EHRs) from all intensive care unit (ICU) stays in MIMIC-III. Each record combines tabular variables and clinical notes describing the patient’s state prior to treatment. We define a reference time t_0 three hours after ICU admission and a follow-up window Δt of six hours. All covariates are derived from data recorded up to t_0 ; the treatment is defined within the interval $(t_0, t_0 + \Delta t)$; and the outcome is measured after $t_0 + \Delta t$. ICU stays that end before $t_0 + \Delta t$ are excluded. As tabular variables in the EHR, we retain the demographic attributes age and sex, consistent with the previous datasets. We exclude individuals younger than 18 years and retain only the first ICU stay of each patient. All clinical notes recorded before t_0 are extracted and concatenated into a single text sequence representing the documentation available to clinicians at the time of treatment decision. Each resulting EHR therefore consists of the tabular demographic variables age and sex and an aggregated

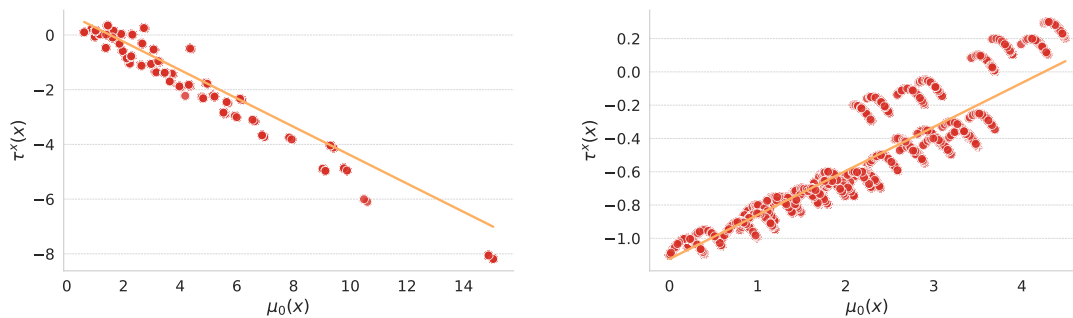
clinical note summarizing the patient’s condition prior to treatment. In the following paragraphs, we describe the construction of the treatment and outcome variables.

Treatment and Outcome. The treatment variable $T \in \{0, 1\}$ indicates whether at least one antibiotic prescription was administered during the interval $(t_0, t_0 + \Delta t)$. Antibiotic prescriptions are identified using a curated list of antibiotic drug names. The outcome variable $Y \in \{0, 1\}$ denotes in-hospital mortality occurring after $t_0 + \Delta t$, reflecting post-treatment mortality between the end of the treatment window and hospital discharge.

In the resulting dataset (8,685 ICU stays), 18.5% of patients received antibiotics within the treatment window ($T=1$), and 12.0% died after the treatment window during the same hospitalization ($Y=1$). Mortality was 16.4% among treated patients and 11.0% among untreated patients. This higher mortality among treated patients does not indicate a harmful treatment effect but reflects confounding: antibiotics are typically administered to patients with suspected sepsis or severe infection, who are inherently at higher risk of death. Consequently, treatment and outcome are strongly associated through shared confounders such as abnormal vital signs and infection-related findings, underscoring the importance of causally informed treatment assignment strategies.

Feature Representations. Each EHR in MIMIC-REAL consists of the tabular demographic variables (age and sex) and an aggregated clinical note describing the patient’s condition prior to treatment. We encode the clinical text using the pretrained language model ModernBERT (Warner et al., 2024), mean-pool the token embeddings, and concatenate the resulting text representation with the tabular variables to obtain the multimodal representation ϕ . This representation captures both explicit demographic information and implicit clinical signals present in the real-world EHR data.

Confounding Annotations. In this real-world setting, we assume that vital signs can act as confounders for antibiotic administration and mortality. Clinicians are more likely to prescribe antibiotics to patients presenting with ab-



(a) **SynSum.** Relationship between $\mu_0(x)$ and $\tau^x(x)$. The association is negative, indicating that patients with higher baseline risk exhibit larger treatment benefit.

(b) **MIMIC-Syn.** Relationship between $\mu_0(x)$ and $\tau^x(x)$. The association is positive, showing that patients with higher baseline risk experience reduced treatment benefit. The oscillations visible in the right subplot arise from the sinusoidal age term in $\tau^x(x)$.

Figure 5: Relationship between the true baseline risk $\mu_0(x)$ and the true treatment effect $\tau^x(x)$ across synthetic datasets. In **SynSum** (left), the relationship is negative: patients with higher baseline risk tend to experience greater treatment benefit (more negative effects). In contrast, in **MIMIC-Syn** (right), the relationship is positive: treatment benefit attenuates as baseline risk increases. The oscillations visible in the right subplot arise from the sinusoidal age term in $\tau^x(x)$.

normal physiologic measurements (such as fever, tachycardia, or hypotension) which also indicate higher mortality risk. These vital sign readings (temperature, heart rate, respiratory rate, oxygen saturation, systolic blood pressure, and mean arterial pressure) are available as structured variables in MIMIC-III, and we extracted them for each patient prior to treatment (before t_0).

To assess whether this confounding information is implicitly expressed in the clinical text, we evaluated how well abnormal vital sign patterns can be predicted from the text representations. Vital signs were discretized according to standard clinical thresholds: fever (temperature $\geq 37.5^\circ\text{C}$), hypothermia (temperature $\leq 35.5^\circ\text{C}$), tachycardia (heart rate ≥ 100 beats pm.), tachypnea (respiratory rate ≥ 22 breaths pm.), hypoxemia (oxygen saturation $< 92\%$), and hypotension (mean arterial pressure < 65 mmHg or systolic blood pressure < 90 mmHg). Each abnormality indicator was then predicted using only the ModernBERT text embeddings. The dataset was randomly divided into 80% training, 10% validation, and 10% test splits.

As shown in Table 4, these physiological states are predictable from the clinical text (substantially better than random chance since all AU-

ROC values > 0.5), confirming that confounding information is implicitly encoded in the notes. Consequently, we use the continuous vital sign measurements as expert-provided confounding annotations during training of the causal model. At inference time, these models rely solely on the multimodal representations ϕ . We note, however, that this dataset may still contain unobserved confounding factors beyond the available vital sign measurements.

B.4. Summary

In summary, the three datasets (SYNSUM, MIMIC-SYN, and MIMIC-REAL) enable evaluation of the risk-based and causal treatment assignment strategies across settings that range from purely synthetic simulations to real-world clinical data. In the following section, we present detailed experimental results and analyses based on these datasets.

Table 4: Prediction of physiological confounders from pre- t_0 clinical notes in the MIMIC-REAL dataset (mean \pm std over 5 random seeds). ‘‘Prev.’’ denotes the positive-class prevalence in the test set. Each classifier’s decision threshold was selected to maximize F1 score on the validation set.

Confounder	Prev.	F1	Acc.	AUPRC	AUROC
Fever	0.14	0.337 ± 0.007	0.607 ± 0.026	0.253 ± 0.003	0.680 ± 0.003
Hypothermia	0.04	0.026 ± 0.041	0.951 ± 0.013	0.097 ± 0.026	0.649 ± 0.024
Tachycardia	0.22	0.435 ± 0.006	0.617 ± 0.021	0.381 ± 0.002	0.679 ± 0.003
Tachypnea	0.26	0.467 ± 0.006	0.599 ± 0.025	0.408 ± 0.004	0.678 ± 0.005
Hypoxemia	0.03	0.111 ± 0.012	0.746 ± 0.093	0.118 ± 0.006	0.629 ± 0.010
Hypotension (MAP)	0.17	0.343 ± 0.006	0.539 ± 0.011	0.278 ± 0.011	0.636 ± 0.007
Hypotension (SBP)	0.06	0.200 ± 0.013	0.790 ± 0.017	0.130 ± 0.004	0.714 ± 0.006

Appendix C. Experimental Results

This section presents the empirical evaluation of the considered treatment assignment strategies across the three datasets introduced in Appendix B. We begin with the fully synthetic SYN-SUM dataset, then examine performance on the semi-synthetic MIMIC-SYN dataset in a realistic yet partially simulated setting. Finally, we provide a qualitative comparison on the real-world MIMIC-REAL dataset, where both treatments and outcomes are observed from clinical practice. For completeness, some results reported in the main paper are repeated here so that the appendix can be read independently.

C.1. Results on SynSum

Confounder Signal in Text. To verify that the representations of the clinical notes capture confounding information, we trained supervised classifiers to predict each confounder (e.g., fever, cough, dyspnea) directly from the ModernBERT text embeddings. The classifiers were trained on 80% of the data, with 10% used for validation and 10% for testing. As shown in Table 5, the classifiers achieve near-perfect discrimination across all symptom confounders (AUROC $>$ 0.93), indicating that the text representations almost completely recover the underlying confounding information. This property of the SYN-SUM dataset confirms that the representations encode the relevant confounding signal, motivating their suitability for downstream treatment effect estimation.

Coarsened Treatment Effect Quality. To evaluate how well the coarsened treatment effects can be learned in SYN-SUM, we trained models to estimate these effects using varying amounts of training data and measured their accuracy using the PEHE (precision in estimation of heterogeneous effects - lower is better), which is defined as the root mean squared error between the estimated and true treatment effects. We trained the second-stage treatment effect models in three scenarios: using the true confounders, the multimodal representations (text + tabular) and the tabular variables only as inputs. Each experiment used 10% of the data for validation and 10% for testing.

As shown in Figure 6, PEHE decreases consistently with increasing training size. As expected, estimators based on true confounders perform best, followed by the models trained on multimodal representations (text + tabular) and tabular variables only. This indicates that while multimodal representations introduce some coarsening, they capture substantial confounding information relevant for treatment effect estimation.

Treatment Policy Evaluation. We next compare the causal and risk-based treatment policies on the SYN-SUM benchmark. Both approaches are evaluated in their oracle form (ranking by the true treatment effect or baseline risk) and as learned models trained on varying amounts of data. Table 6 summarizes the corresponding policy metrics, while Figure 7 shows the AUROC trends across training sizes.

Table 5: Prediction of symptom confounders from clinical notes in the SYN SUM dataset (mean \pm std over 5 random seeds). “Prev.” denotes the positive-class prevalence in the test set. Each classifier’s decision threshold was selected to maximize F1 score on the validation set.

Confounder	Prev.	F1	Acc.	AUPRC	AUROC
Cough	0.36	0.971 \pm 0.001	0.979 \pm 0.001	0.989 \pm 0.000	0.991 \pm 0.000
Dyspnea	0.20	0.949 \pm 0.010	0.980 \pm 0.004	0.980 \pm 0.001	0.990 \pm 0.001
Fever (high)	0.07	0.995 \pm 0.007	0.999 \pm 0.001	1.000 \pm 0.000	1.000 \pm 0.000
Fever (low)	0.17	0.841 \pm 0.006	0.951 \pm 0.002	0.879 \pm 0.001	0.935 \pm 0.000
Fever (none)	0.77	0.968 \pm 0.001	0.950 \pm 0.002	0.983 \pm 0.000	0.956 \pm 0.001
Nasal symptoms	0.25	0.974 \pm 0.001	0.987 \pm 0.000	0.984 \pm 0.000	0.990 \pm 0.000
Pain	0.15	0.796 \pm 0.014	0.950 \pm 0.003	0.851 \pm 0.006	0.930 \pm 0.004

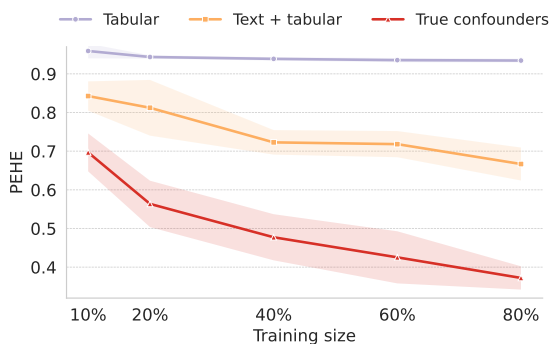


Figure 6: Precision in estimation of heterogeneous effects (PEHE) on the SYN SUM dataset as a function of training set size (mean \pm std over 5 random seeds). The second-stage treatment effect models were trained and evaluated with the true confounders, the multimodal representations (text + tabular) and the tabular variables only as inputs.

On SYN SUM, the causal and risk-based policies exhibit very similar performance across all data regimes, gradually approaching their respective oracle values as the amount of training data increases. This convergence results from the strong negative correlation between baseline risk ($\mu_0(x)$) and treatment benefit ($\tau^x(x)$) in the data generating process (see Appendix B.1, Fig. 5). Patients at higher risk under no treatment also gain most from treatment, so ranking by either criterion leads to nearly identical treatment allocation. At the smallest training sizes, the risk-based strategy even slightly outperforms the

causal one, reflecting that risk prediction can be easier than treatment effect estimation in finite samples. As the sample size grows, the causal policy catches up, and both converge toward the same performance ceiling defined by their oracles. Overall, these results indicate that when risk and benefit are aligned, as in SYN SUM, risk-based policies can appear competitive, but their success relies on this specific property of the data.

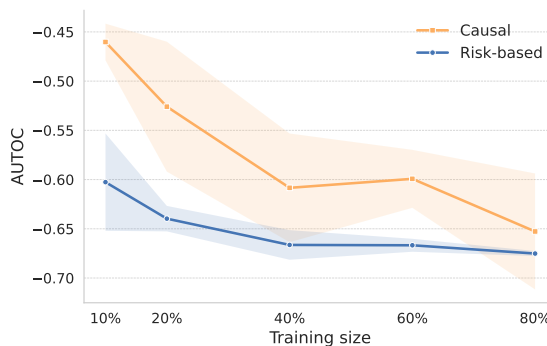


Figure 7: AUROC of the causal and risk-based policies on the SYN SUM dataset as a function of training set size (mean \pm std over 5 random seeds). Lower (more negative) AUROC values indicate better ranking quality. Both policies improve with increasing data, and for sufficiently large training sizes, the two strategies yield nearly identical treatment allocations.

Table 6: Policy evaluation metrics for the causal and risk-based models on the SYN-SUM dataset (mean \pm std over five random seeds). Lower policy values (indicated as \bar{V} for mean policy value over all thresholds, and $V_{10\%}$ at the 10% threshold) and more negative AUROC indicate better performance. The best model within each training size is shown in **bold**, unless the difference was not significant at the 5% level based on a two-sided t -test. The ‘oracle’ rows report policies ranking by the true treatment effect (causal) or the untreated outcome (risk-based).

Training size	Model	AUROC (\downarrow)	\bar{V} (\downarrow)	$V_{5\%}$ (\downarrow)	$V_{10\%}$ (\downarrow)
10%	Causal	-0.46 ± 0.02	1.764 ± 0.005	1.948 ± 0.007	1.874 ± 0.009
	Risk-Based	-0.60 ± 0.05	1.750 ± 0.004	1.889 ± 0.009	1.825 ± 0.014
20%	Causal	-0.53 ± 0.07	1.757 ± 0.010	1.929 ± 0.019	1.851 ± 0.022
	Risk-Based	-0.64 ± 0.01	1.747 ± 0.001	1.884 ± 0.002	1.816 ± 0.006
40%	Causal	-0.61 ± 0.06	1.747 ± 0.005	1.905 ± 0.018	1.822 ± 0.015
	Risk-Based	-0.67 ± 0.02	1.746 ± 0.002	1.878 ± 0.002	1.812 ± 0.006
60%	Causal	-0.60 ± 0.03	1.747 ± 0.004	1.910 ± 0.015	1.825 ± 0.011
	Risk-Based	-0.67 ± 0.01	1.745 ± 0.001	1.877 ± 0.002	1.813 ± 0.004
80%	Causal	-0.65 ± 0.06	1.742 ± 0.003	1.891 ± 0.021	1.814 ± 0.018
	Risk-Based	-0.68 ± 0.00	1.745 ± 0.000	1.874 ± 0.003	1.812 ± 0.002
Oracle	Causal	-0.88	1.697	1.847	1.766
	Risk-Based	-0.81	1.724	1.847	1.784

C.2. Results on MIMIC-Syn

Confounder Signal in Text. To assess whether the representations of the clinical notes capture confounding information in the semi-synthetic MIMIC-SYN dataset, we trained supervised classifiers to predict each cardiovascular confounder (hypertension, coronary atherosclerosis, atrial fibrillation, and congestive heart failure) directly from the ModernBERT embeddings. Models were trained on 80% of the data, with 10% used for validation and 10% for testing. As shown in Table 7, the classifiers achieve good discrimination across all confounders (AUROC ranging from 0.69 to 0.92), confirming that the text representations encode meaningful information about the latent cardiovascular conditions. This motivates their use for downstream treatment effect estimation in a realistic, partially observed setting.

Coarsened Treatment Effect Quality. To evaluate the learnability of the coarsened treatment effects in MIMIC-SYN, we trained models to estimate these effects using varying amounts of

training data and measured their accuracy using PEHE. We again included second-stage models in three scenarios: using the true confounders, the multimodal representations (text + tabular) and the tabular variables only as input, and each experiment used 10% of the data for validation and 10% for testing.

As shown in Figure 8, PEHE decreases consistently with increasing training size across inputs. The true confounder-based estimators perform best, followed by the models trained on the multimodal representations (text + tabular) and the tabular variables only. The multimodal representation-based models (text + tabular) again demonstrate robust improvement as more annotated data becomes available.

Treatment Policy Evaluation. We now compare the causal and risk-based policies on the MIMIC-SYN dataset, both in their oracle form (ranking by the true treatment effect or baseline risk) and as learned models trained on varying amounts of data. Table 8 summarizes the policy evaluation metrics across training sizes.

Table 7: Prediction of diagnostic confounders from clinical notes in the MIMIC-SYN dataset (mean \pm std over 5 random seeds). “Prev.” denotes the positive-class prevalence in the test set. Each classifier’s decision threshold was selected to maximize F1 score on the validation set.

Confounder	Prev.	F1	Acc.	AUPRC	AUROC
Atrial fibrillation	0.24	0.694 \pm 0.007	0.856 \pm 0.005	0.759 \pm 0.004	0.889 \pm 0.002
Congestive heart failure	0.22	0.591 \pm 0.005	0.794 \pm 0.009	0.584 \pm 0.004	0.845 \pm 0.002
Coronary atherosclerosis	0.26	0.766 \pm 0.003	0.884 \pm 0.006	0.854 \pm 0.004	0.917 \pm 0.002
Hypertension	0.44	0.648 \pm 0.002	0.573 \pm 0.009	0.615 \pm 0.002	0.694 \pm 0.002

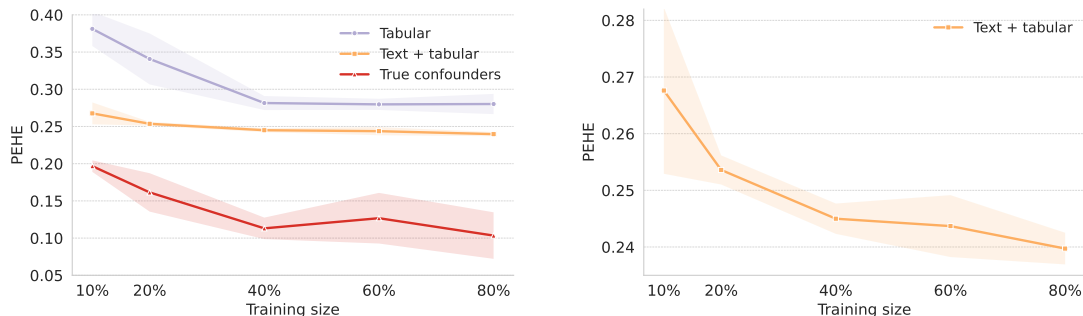


Figure 8: Precision in estimation of heterogeneous effects (PEHE) of the estimators on the MIMIC-SYN dataset as a function of training set size (mean \pm std over 5 random seeds). **Left:** comparison between second-stage models trained and evaluated with the true confounders, multimodal representations (text + tabular) and tabular variables only as input. **Right:** zoomed-in view of the representation-based estimator, highlighting the consistent improvement with increasing data.

In contrast to the SYN SUM setting, where risk and benefit were aligned, MIMIC-SYN exhibits a strong *positive* correlation between baseline risk ($\mu_0(x)$) and treatment effect ($\tau^x(x)$): patients at higher baseline risk tend to benefit less from treatment (see Appendix B.2, Fig. 5). As a result, the risk-based policy systematically prioritizes individuals with low expected benefit, yielding substantially worse policy values than the causal policy. In contrast, the causal policy improves steadily with increasing data and approaches its oracle performance already at moderate sample sizes. These results highlight that when baseline risk and treatment benefit are misaligned, causal policy learning is essential for effective treatment allocation, whereas risk-based strategies may lead to suboptimal treatment decisions even with accurate risk models.

C.3. Summary of Synthetic Evaluation.

Taken together, the experiments on SYN SUM and MIMIC-SYN show that coarsened treatment effects can be learned reliably given high-quality confounder annotations, and that causal treatment policies can be derived effectively from multimodal EHR representations that partially capture confounding information. Across both datasets, causal policy learning consistently outperforms risk-based strategies once sufficient data is available. The contrast between the two settings highlights the role of the underlying risk-benefit relationship: when risk and benefit are aligned (SYN SUM), both strategies perform similarly, whereas when they diverge (MIMIC-SYN), only the causal policy yields effective treatment allocation.

Table 8: Policy evaluation metrics for the causal and risk-based models on the MIMIC-SYN dataset (mean \pm std over five random seeds). Lower values indicate better performance, consistent with the interpretation in Table 6.

Training size	Model	AUROC (\downarrow)	\bar{V} (\downarrow)	$V_{5\%}$ (\downarrow)	$V_{10\%}$ (\downarrow)
10%	Causal	-0.13 ± 0.01	1.055 ± 0.002	1.417 ± 0.001	1.369 ± 0.002
	Risk-Based	0.16 ± 0.00	1.148 ± 0.001	1.448 ± 0.001	1.425 ± 0.001
20%	Causal	-0.14 ± 0.00	1.051 ± 0.002	1.417 ± 0.000	1.368 ± 0.001
	Risk-Based	0.17 ± 0.00	1.149 ± 0.001	1.449 ± 0.001	1.427 ± 0.001
40%	Causal	-0.14 ± 0.00	1.049 ± 0.001	1.417 ± 0.000	1.368 ± 0.001
	Risk-Based	0.17 ± 0.00	1.150 ± 0.000	1.450 ± 0.000	1.428 ± 0.001
60%	Causal	-0.14 ± 0.00	1.048 ± 0.001	1.417 ± 0.000	1.368 ± 0.000
	Risk-Based	0.17 ± 0.01	1.151 ± 0.001	1.449 ± 0.001	1.428 ± 0.002
80%	Causal	-0.14 ± 0.00	1.047 ± 0.001	1.417 ± 0.000	1.368 ± 0.000
	Risk-Based	0.18 ± 0.00	1.152 ± 0.001	1.449 ± 0.000	1.429 ± 0.000
Oracle	Causal	-0.20	1.020	1.413	1.362
	Risk-Based	0.28	1.172	1.468	1.450

C.4. Results on MIMIC-Real

Confounder Signal in Text. As detailed in Appendix B.3, we verified that the clinical text in MIMIC-REAL encodes confounding information related to physiological states such as fever, tachycardia, and hypotension. Predictive models trained on ModernBERT embeddings achieved AUROC values between 0.63 and 0.71 across all vital-sign confounders (Table 4), confirming that this information is recoverable from the notes. These findings support the use of the representations for evaluating causal treatment assignment strategies in real-world EHR data.

Qualitative Comparison of Treatment Assignments. In the MIMIC-REAL dataset, where only observational outcomes are available, we qualitatively compare the treatment recommendations generated by the causal and risk-based policies and examine their alignment with real-world antibiotic prescribing. The dataset was randomly divided into 80% training, 10% validation, and 10% test splits.

Table 9 shows that the overlap between the causal and risk-based recommendations is highly limited: for instance, only about 25% of patients in the top 20% treated by either policy are

shared, indicating that the two strategies prioritize largely distinct patient subsets.

Table 10 further compares each strategy’s recommendations with the observed prescription policy. Both models exhibit modest overlap with real-world treatment allocation, reflecting that model-based prioritization differs substantially from existing clinical practice. The risk-based policy, however, shows somewhat higher alignment with the observed prescriptions than the causal policy.

We additionally assessed the stability of each treatment assignment strategy by computing the correlation between the patient-level treatment ranks obtained from different random seeds on the test set. Across seeds, both the weight initialization and data sampling varied. Both policies demonstrated stable behaviour, with average correlations of $\rho = 0.62 \pm 0.30$ for the causal strategy and $\rho = 0.99 \pm 0.01$ for the risk-based strategy, indicating that the learned prioritizations are largely reproducible across runs. Overall, these analyses show that the causal and risk-based strategies yield substantially different treatment assignments from each other and from the observed antibiotic prescription policy.

Table 9: Agreement in treatment recommendations between the causal and risk-based policies on the MIMIC-REAL dataset (mean \pm std over five random seeds). Each value reports the percentage of patients jointly prioritized by both policies at a given top- k % treatment budget, with higher values indicating higher agreement in treatment prioritization.

Top- k (%)	Agreement (%) (Causal vs. Risk-based)
$k = 5$	5.0 ± 7.0
$k = 10$	13.8 ± 8.0
$k = 20$	24.4 ± 7.8
$k = 50$	53.0 ± 5.3
$k = 100$	100.0 ± 0.0

Table 10: Agreement between model-based and observed treatment assignments on the MIMIC-REAL dataset (mean \pm std over five random seeds). The observed policy corresponds to the 20.7% of admissions that actually received antibiotics. For each top- k % treatment budget, we report: (i) the percentage of model-assigned patients who were also treated in practice (*Model* \rightarrow *Observed*), and (ii) the percentage of observed treatments that were also prioritized by the model (*Observed* \rightarrow *Model*). Higher values indicate stronger alignment with real-world prescribing patterns.

Top- k (%)	Causal	Observed	Risk-based	Observed
	\rightarrow Observed (%)	\rightarrow Causal (%)	\rightarrow Observed (%)	\rightarrow Risk-based (%)
$k = 5$	17.2 ± 2.1	4.1 ± 0.5	20.0 ± 1.3	4.8 ± 0.3
$k = 10$	16.1 ± 1.6	7.8 ± 0.8	17.7 ± 2.1	8.6 ± 1.0
$k = 20$	14.6 ± 3.8	14.1 ± 3.7	21.5 ± 0.8	20.8 ± 0.7
$k = 50$	18.0 ± 1.5	43.3 ± 3.6	22.9 ± 0.5	55.3 ± 1.3
$k = 100$	20.7 ± 0.0	100.0 ± 0.0	20.7 ± 0.0	100.0 ± 0.0

Appendix D. Experimental Details

This section provides implementation details common to all experiments. Unless stated otherwise, the same architecture, hyperparameter tuning procedure, and early stopping strategy were used across all datasets and model components. All experiments were conducted on a machine equipped with one NVIDIA GeForce GTX 2080 GPU. Training was computationally lightweight, with most models converging in under 10 minutes.

Model Architecture. All models (classifiers, nuisance models, and treatment effect regressors) were implemented as small neural networks consisting of a single hidden layer with ReLU activations. The output layer was sigmoid for binary classification tasks (e.g., propensity estimation,

confounder prediction) and linear for regression tasks (e.g., outcome and treatment effect estimation).

Training Setup. All models were trained using the Adam optimizer with optional weight decay and a maximum of 50 epochs. Early stopping based on the validation loss (patience of 5 epochs) was applied, retaining the parameters corresponding to the best validation performance. For confounder prediction tasks, we used class-weighted binary cross-entropy loss, with the positive class weight set to $(1 - p)/p$, where p is the positive-class prevalence in the training set. Other classification tasks used standard binary cross-entropy loss, and regression tasks used mean squared error loss.

Hyperparameter Tuning. Hyperparameters were tuned once per model family on an intermediate training size (40% of the available data) and then reused for all experiments with varying training set sizes. We performed a random search of 12 trials over the following grid: hidden dimension $\in \{64, 128\}$, learning rate $\in \{10^{-4}, 3 \times 10^{-4}, 5 \times 10^{-4}, 10^{-3}\}$, weight decay $\in \{0, 10^{-5}, 10^{-4}\}$, and batch size $\in \{128, 256\}$. The configuration achieving the lowest validation loss was selected and applied across all random seeds.

Data Splits. All experiments used 10% of the data for validation and 10% for testing. The remaining portion was used for training, with the fraction varying depending on the experiment (e.g., 10%, 20%, 40%, 60%, or 80% of the full dataset). Random seeds affected both data splits and weight initialization.

Cross-Fitting. We do not apply cross-fitting when constructing the doubly robust pseudo-outcomes. This design choice reflects our focus on comparing causal and risk-based treatment strategies rather than on achieving asymptotic efficiency. In small to medium sample regimes such as those considered here, omitting cross-fitting simplifies implementation and computation while the impact on the relative performance trends between models is limited.